**Supporting Information**

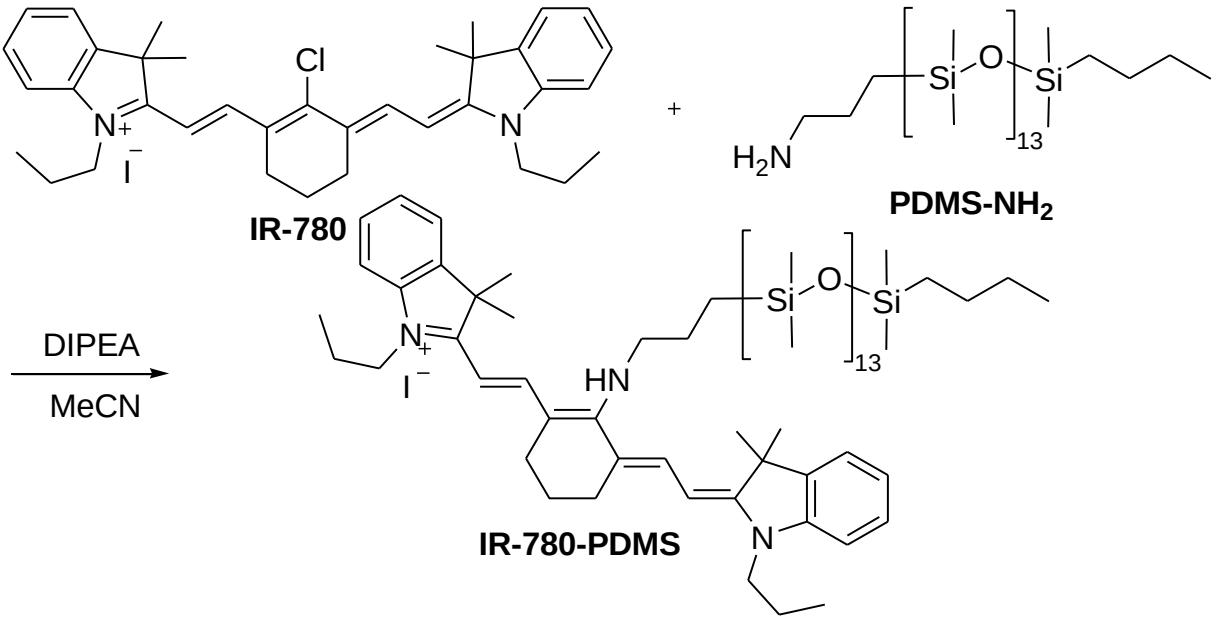


Figure S1. Synthesis of IR-780-PDMS. Reaction Conditions: DIPEA, MeCN, refluxing.

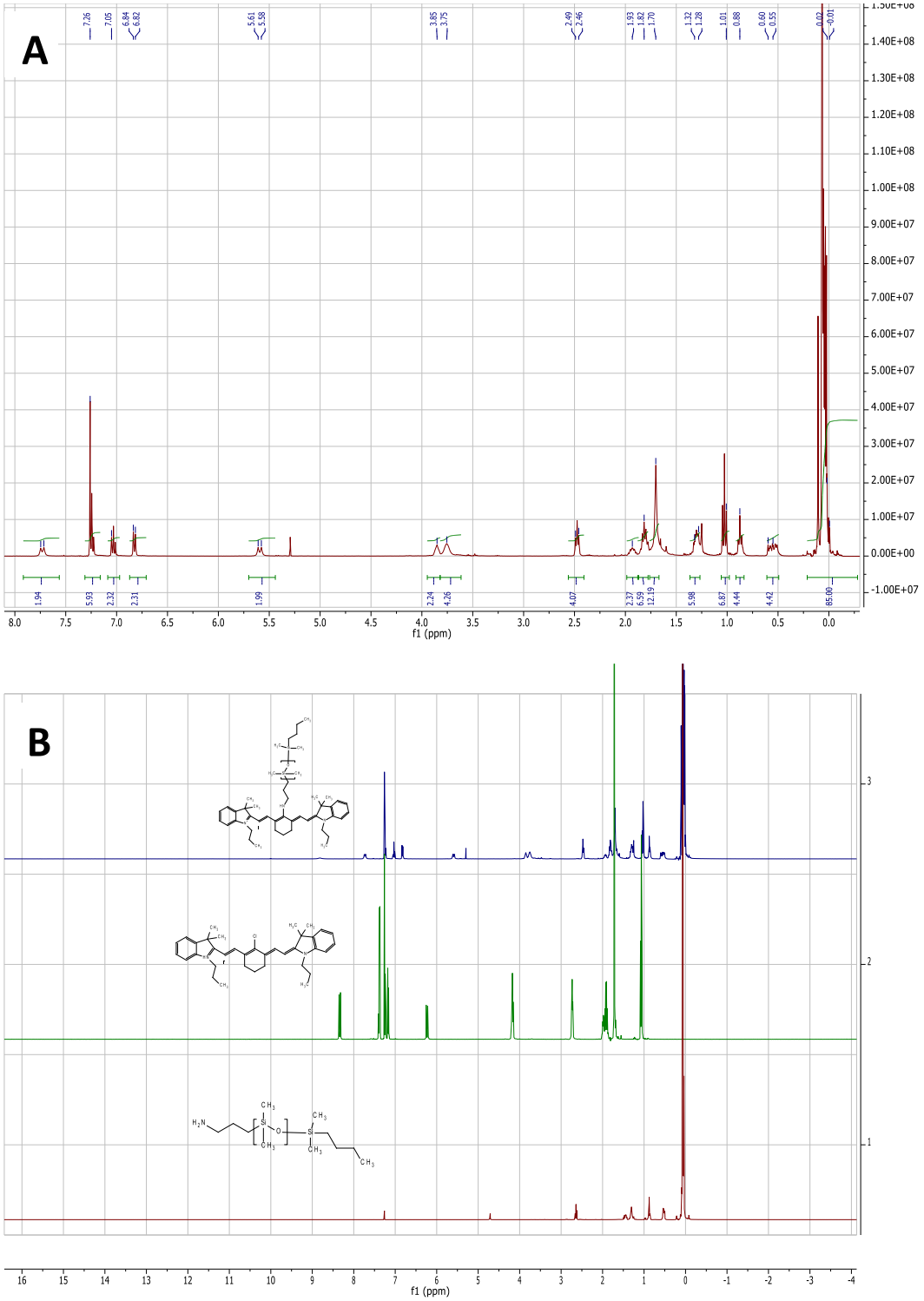


Figure S2. (A) $^{1}$H NMR spectrum of compound IR-780-PDMS ($CDCl_3$ as solvent), (B) $^{1}$HNMR Comparison of IR780-PDMS, IR-780, and PDMS-$NH_2$ ($CDCl_3$ as solvent).

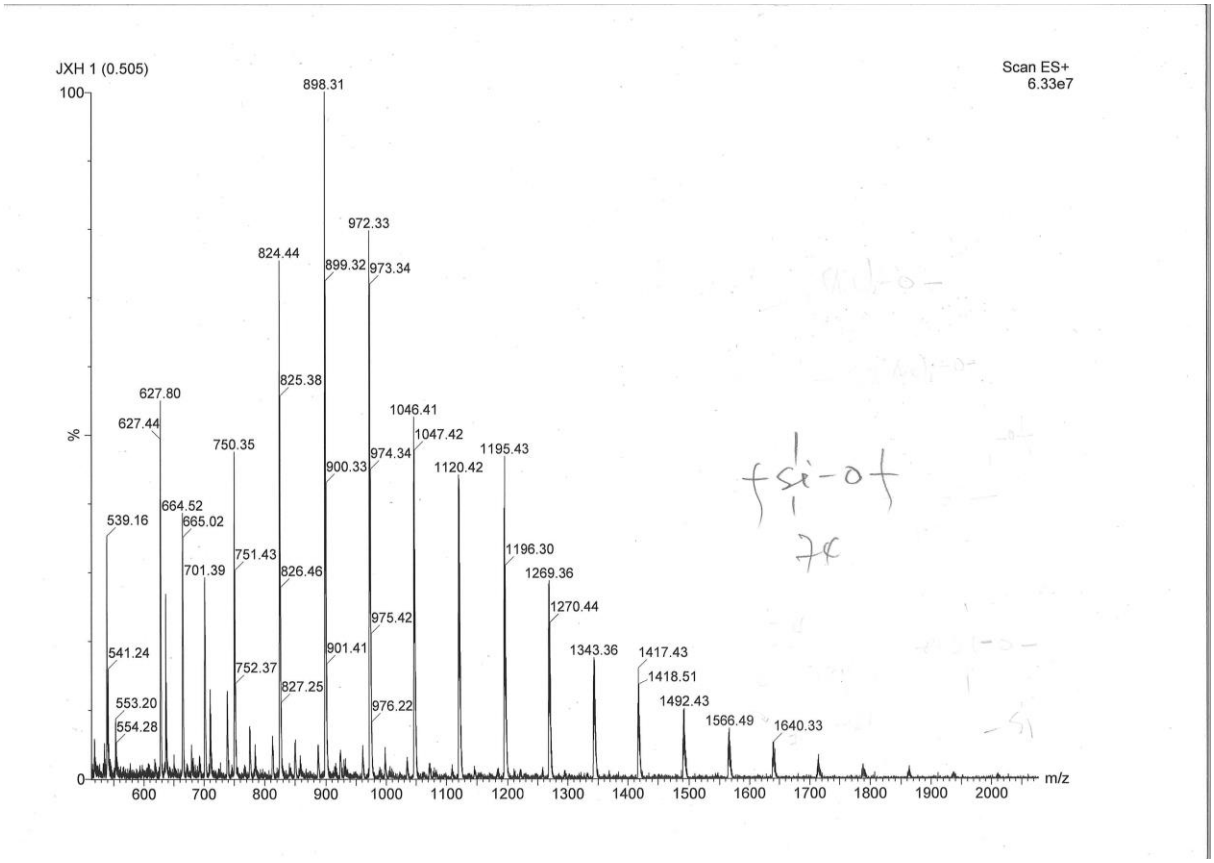


Figure S3. ESI-spectrum of IR-780-PDMS. From the ESI-mass spectrum of IR-780-PDMS, we found different signals with a regular interval (74 Dalton) which should be produced by a cleavage of fragment of "–$Si(Me)_2$-O-" from the whole molecule during electrospray ionization (ESI) .

Octanol/water (1:4 in V/V)

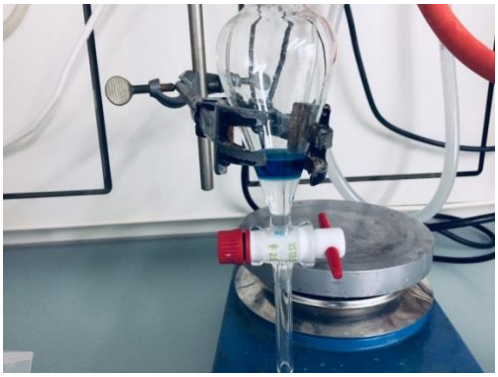

Octanol/water (1:1 in V/V)

Figure S4. IR-780-PDMS in octanol-water system. The dark blue phase is the octanol phase in which the dye IR780-PDMS is dissolved. No colour was found in the aqueous phase (i.e. no dye and no UV-Vis absorption in the aqueous solution could be detected).

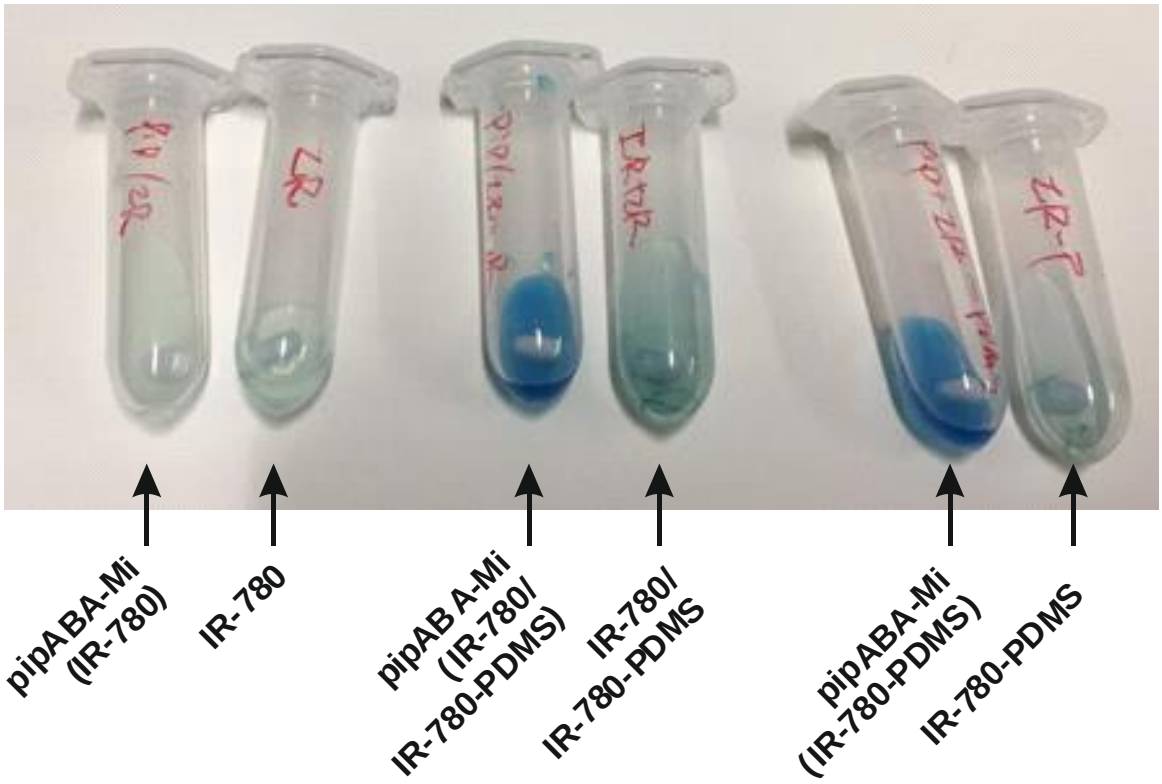


Figure S5. Physical appearance of six different solutions of micelles and dyes. Note: the clear dark blue color means the formation of a homogenous solution [e.g. pipABA-Mi(IR-780/IR-780-PDMS) and pipABA-Mi(IR-780-PDMS)] . In contrast, the free dyes precipitated from the PBS buffer and stuck to the surface of the tubes (IR-780/IR-780-PDMS and IR-780-PDMS) due to their high hydrophobicity.

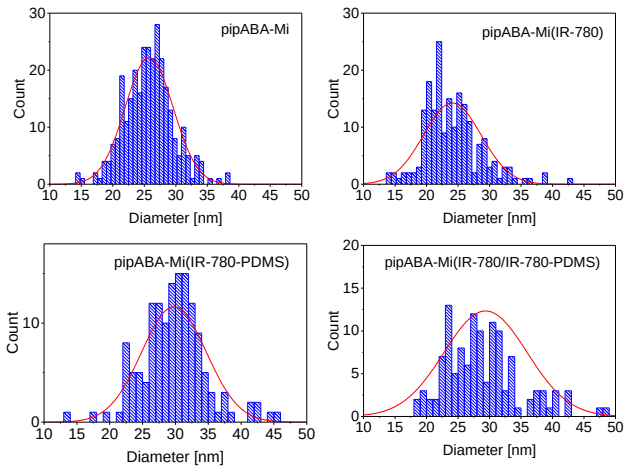

Figure S6. Size distribution of four micelle/dye combinations calculated from TEM measurements with overlaid normal distribution fits.

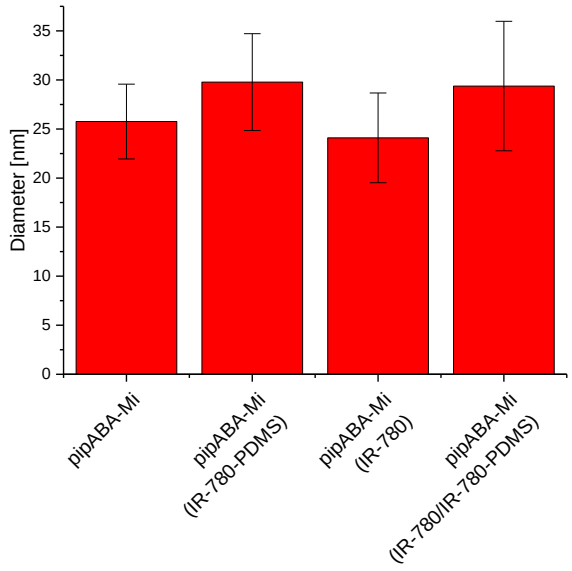


Figure S7. Mean diameter of four different micelle/dye combinations measured from TEM images.

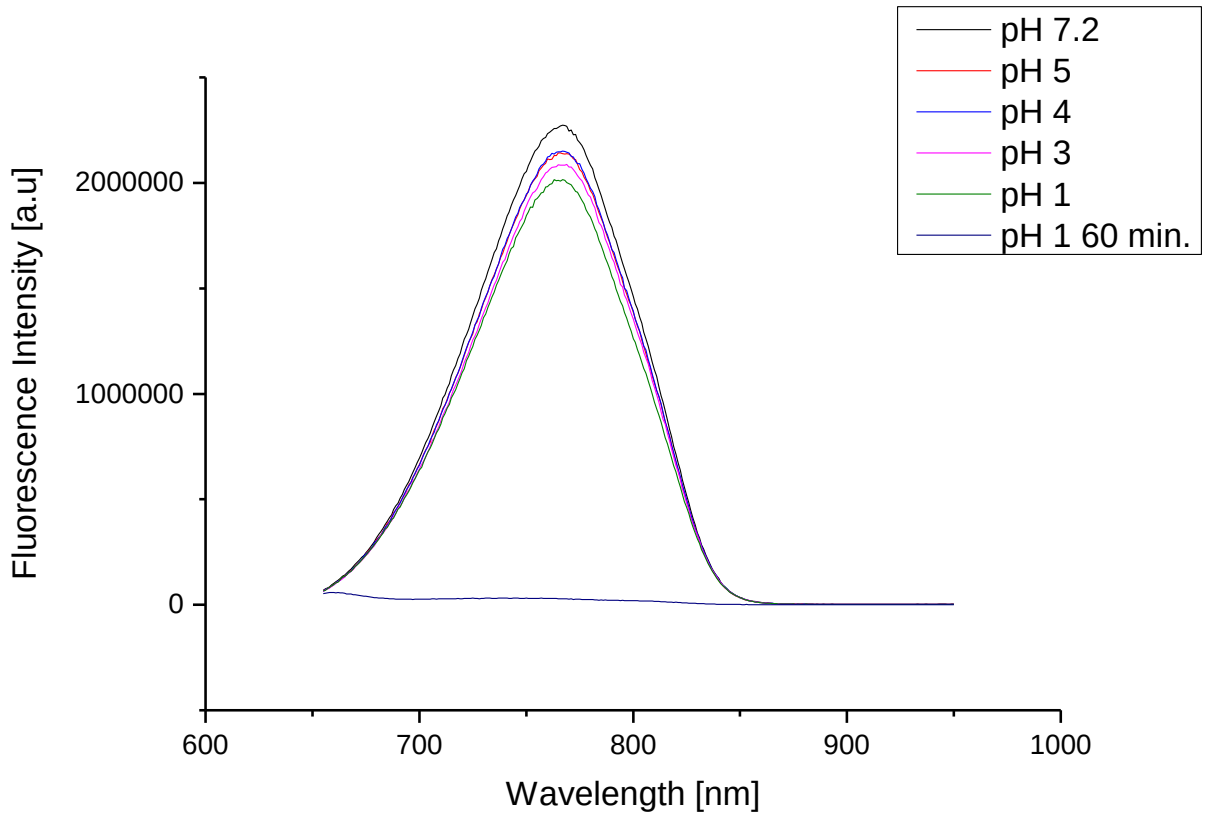

Figure S8. Fluorescence emission spectra of pipABA-Mi(IR-780-PDMS) with excitation wavelength at 640 nm in PBS with different pH values. There was no shift in wavelength. However, after 60 minutes at pH 1, the signal disappeared probably due to decomposition of polymers and/or the dye.

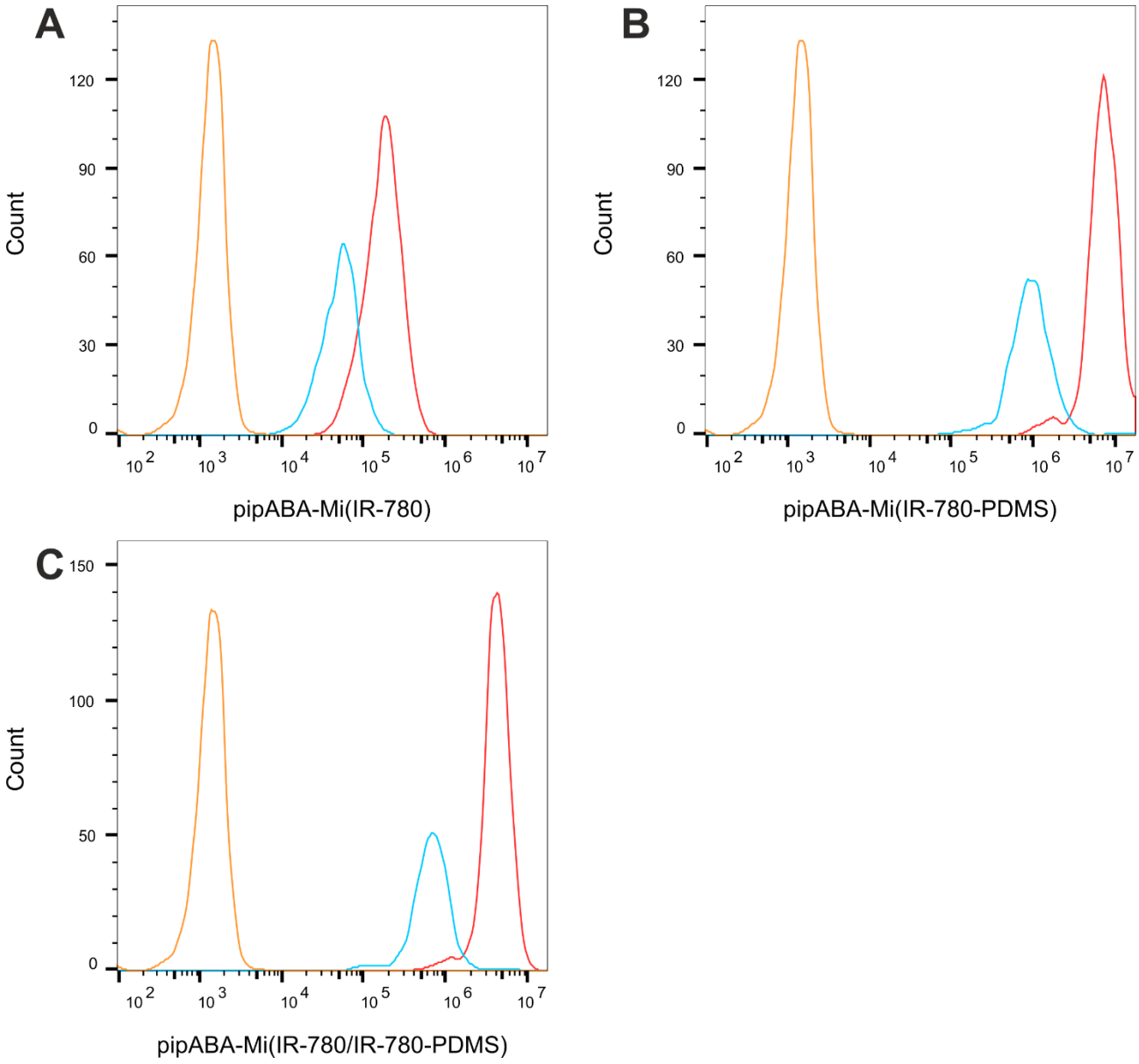


Figure S9. Flow cytometry histograms of HeLa cells treated with 3 different micelle/dye compositions based on the same data as was used in figure 5 in the manuscript. Blue curve: 0.5 h incubation, red curve: 4 hours incubation time, orange curve: negative control (micelles without dye). The mean intensity of (A) is lower than those of (B) and (C), as the excitation wavelength of the flow cytometer (640 nm) lies outside the excitation spectrum of pipABA-Mi(IR-780) and the acquisition band pass is below the emission spectrum of pipABA-Mi(IR-780).

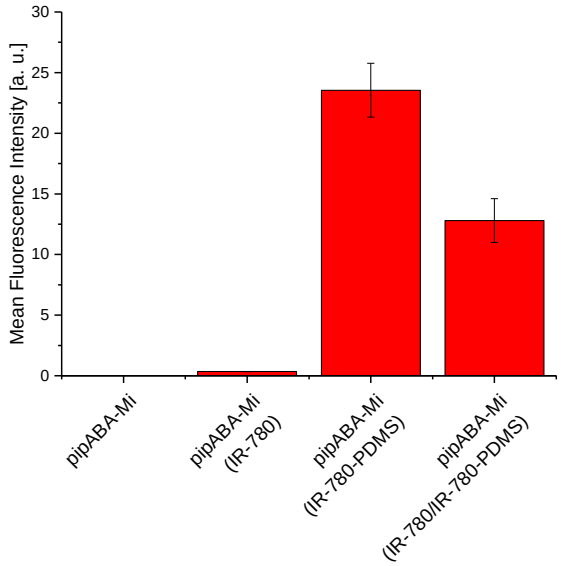


Figure S10. Mean fluorescence intensity of four confocal images in the NIR range. pipABA-Mi (IR-780/IR-780-PDMS) has a lower intensity than pipABA-Mi(IR-780-PDMS), which can be explained by occurrence of FRET, where the emission spectrum of the acceptor (IR-780) is not within the wavelength range of the detector of the microscope.

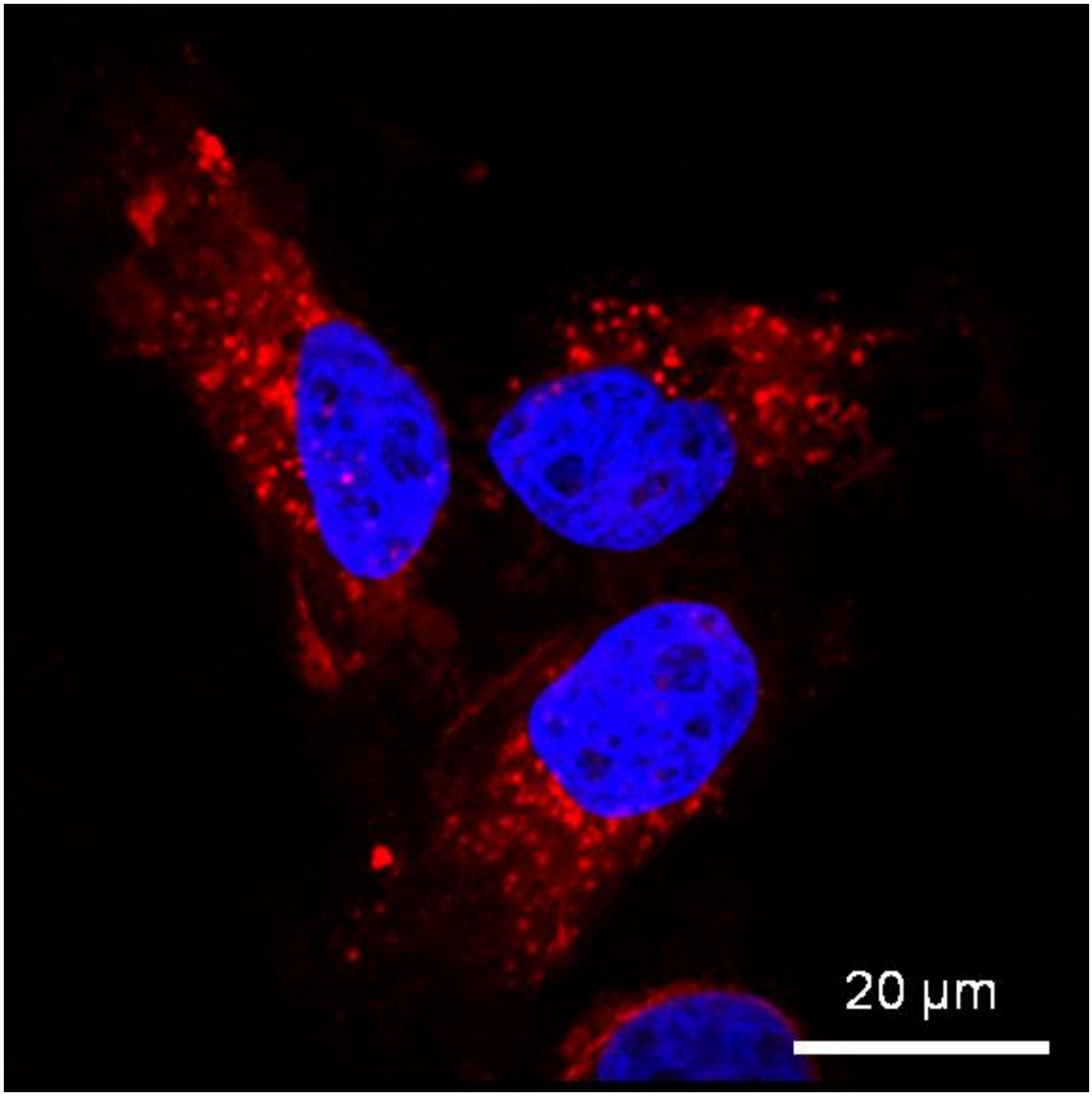


Figure S11. Confocal image of HeLa cells that were incubated with pipABA-Mi(IR-780-PDMS) for 4 h at a magnification of 100 ×.

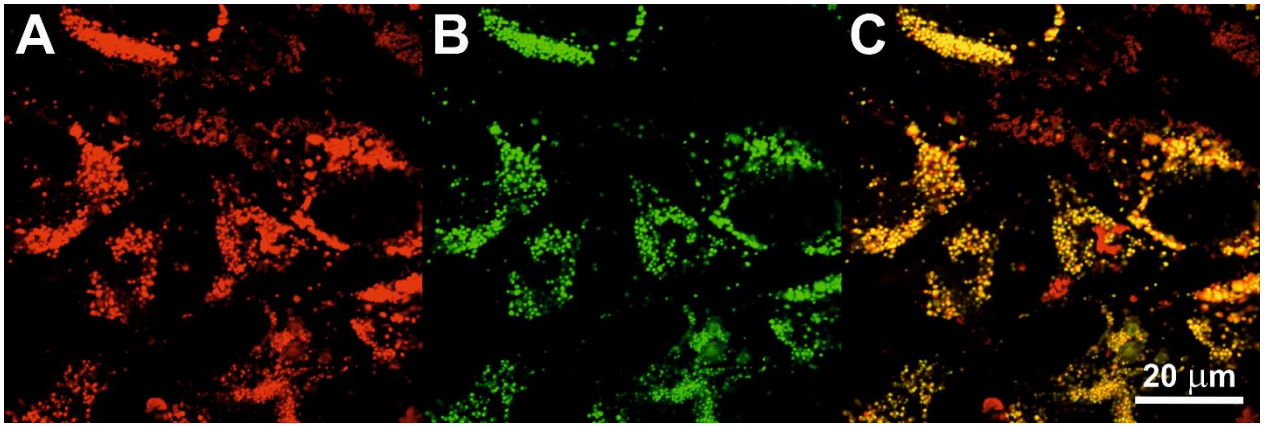


Figure S12. Confocal microscopy images of HeLa cells incubated with Rhodamine B-labelled pipABA-Mi (red, A) for 24 hours and co-incubated with a fluorescent lysosome marker (green, B) for 2 hours. The merged image (C) reveals colocalization of the two dyes (Pearson's R 0.89), confirming lysosomal localization of the uptaken pipABA-Mi.

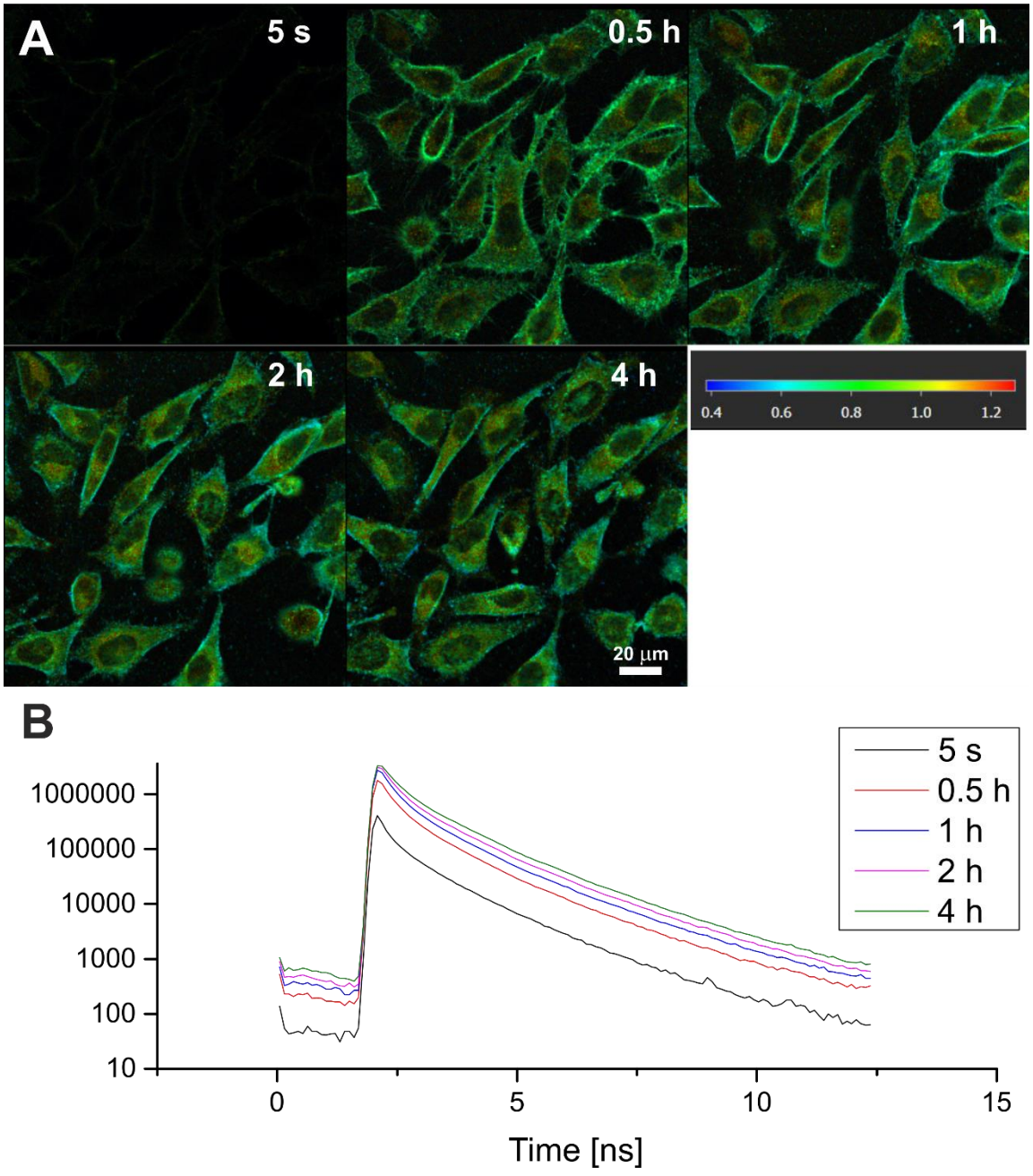


Figure S13. (A) Time series of live HeLa cells incubated with pipABA-Mi(IR-780/IR-780-PDMS) up to 4 hours. (B) Plot of the corresponding fluorescence lifetime decay curves, in which no change in shape or intensity can be observed, except for the one corresponding to an incubation of 5 seconds.

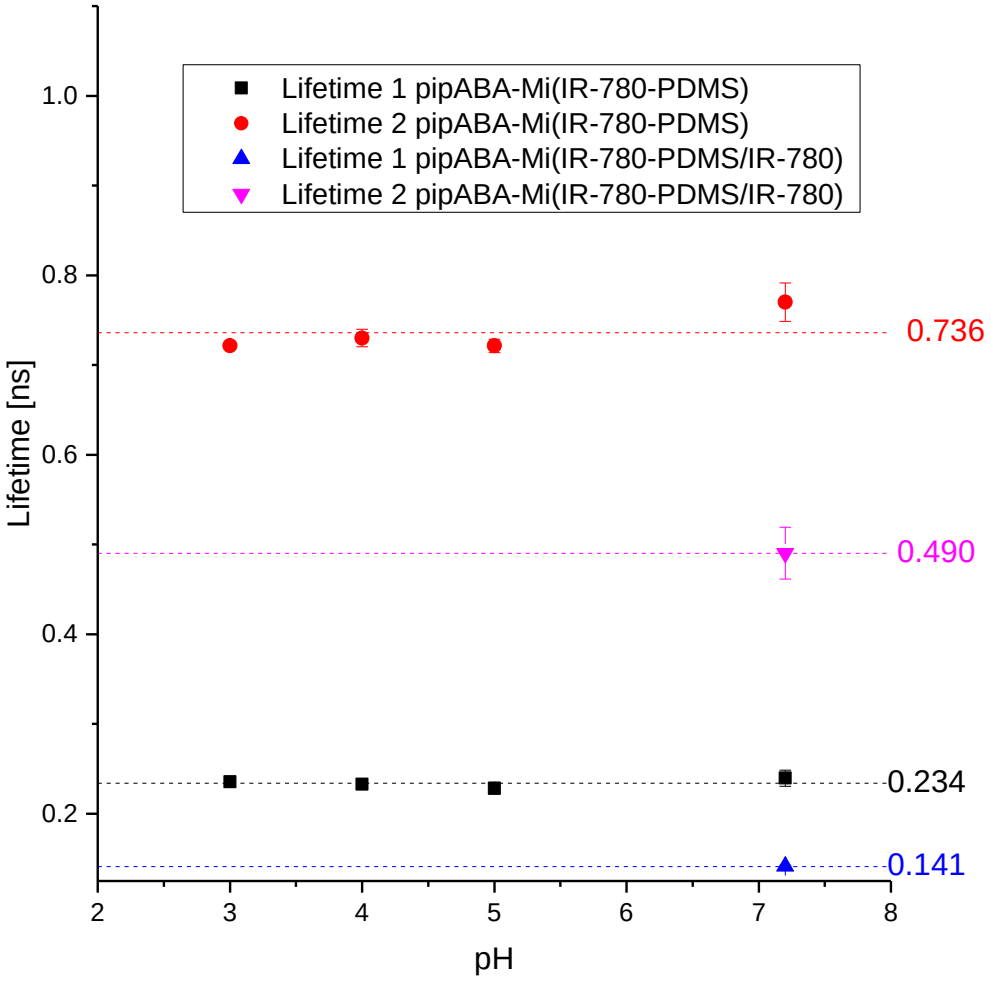


Figure S14. Fluorescence lifetimes of decay curve fits of IR-780-PDMS in pipABA-Mi(IR-780-PDMS) and pipABA-Mi(IR-780/IR-780-PDMS) at different pH values in PBS recorded with FLIM are shown. Lifetimes appear not to respond to changes in pH with a magnitude that is similar to the difference of the donor lifetimes in the quenched and unquenched situation.